P21 Activated Kinase-1 Mediates Transforming Growth Factor β1-Induced Prostate Cancer Cell Epithelial to Mesenchymal Transition

Ahmad Al-Azayzih[1,2], **Fei Gao**[1], and **Payaningal R. Somanath**[1,3,#]

[1]Clinical and Experimental Therapeutics, College of Pharmacy, University of Georgia and Charlie Norwood VA Medical Center, Augusta, GA

[2]College of Pharmacy, Jordan University of Science and Technology, Irbid, Jordan

[3]Department of Medicine, Vascular Biology Center and Cancer Center, Georgia Regents University, Augusta, GA

Abstract

Transforming growth factor beta (TGFβ) is believed to play a dual role in prostate cancer. Molecular mechanism by which TGFβ1 suppresses early prostate tumor growth and induces epithelial-to-mesenchymal transition (EMT) in advanced stages is not known. We determined if P21-activated kinase1 (Pak1), which mediates cytoskeletal remodeling is necessary for the TGFβ1 induced prostate cancer EMT. Effects of TGFβ1 on control prostate cancer PC3 and DU145 cells and those with IPA 3 and siRNA mediated Pak1 inhibition were tested for prostate tumor xenograft *in vivo* and EMT *in vitro*. TGFβ1 inhibited PC3 tumor xenograft growth via activation of P38-MAPK and caspase-3, 9. Long-term stimulation with TGFβ1 induced PC3 and DU145 cell scattering and increased expression of EMT markers such as Snail and N-cadherin through tumor necrosis factor receptor-associated factor-6 (TRAF6)-mediated activation of Rac1/Pak1 pathway. Selective inhibition of Pak1 using IPA 3 or knockdown using siRNA both significantly inhibited TGFβ1-induced prostate cancer cell EMT and expression of mesenchymal markers. Our study demonstrated that TGFβ1 induces apoptosis and EMT in prostate cancer cells via activation of P38-MAPK and Rac1/Pak1 respectively. Our results reveal the potential therapeutic benefits of targeting TGFβ1-Pak1 pathway for advanced-stage prostate cancer.

Keywords

#Corresponding Author: Payaningal R. Somanath Ph.D., FAHA, Center for Pharmacy and Experimental Therapeutics, College of Pharmacy, University of Georgia, HM1200–Georgia Regents University, Augusta, GA 30912; Phone: 706-721-4250; Fax: 706-721-3994; sshenoy@gru.edu.

Conflicts of interest

The authors have declared that no conflicts of interest exist.

1. Introduction

Prostate cancer is one of the most common cancers and is the second leading cause of cancer-related death among men in the United States (Malvezzi et al., 2014; Siegel et al., 2014). Metastatic prostate cancer is very difficult to treat and is the main cause of death among prostate cancer patients (Gupta and Massague, 2006). The mechanism by which prostate cancer cells metastasize to distant organs is not clearly understood. One of the most accepted theories of metastasis is that tumor cells will undergo epithelial to mesenchymal transition (EMT) characterized by induction of mesenchymal markers accompanied with loss of epithelial markers (Nauseef and Henry, 2011; Thiery et al., 2009).

Transforming growth factor beta (TGFβ) is a cytokine that plays a fundamental role in various cellular functions. However, deregulation of TGFβ pathway can lead to various pathological conditions, including cancer (Akhurst and Derynck, 2001; Massague, 2008; Principe et al., 2014). Although studies have demonstrated the tumor suppressive role of TGFβ1 during the early stages of hyperplasia and tumor development, it switches to a tumor promoter during the advanced metastatic stages of cancer (Inman, 2011; Morrison et al., 2013; Principe et al., 2014; Zarzynska, 2014). TGFβ1, the most ubiquitous and best characterized isoform promotes tumor progression and metastasis in advanced cancers utilizing different pathways; both canonical Smad-dependent pathways and non-canonical Smad-independent pathways (Moustakas and Heldin, 2005; Mu et al., 2012; Shi and Massague, 2003). One of the best characterized cellular modifications during EMT in any tissues is the increased expression of mesenchymal cell-surface markers such as N-cadherin and Snail (Gheldof and Berx, 2013; Smith and Odero-Marah, 2012) and loss of epithelial markers such as E-cadherin and cytokeratins (Gheldof and Berx, 2013; Kokkinos et al., 2007). Thus, EMT is a pre-requisite for the advanced stage cancer cells to gain the invasive characteristics. Whereas TGFβ1 activity is well known to be associated with EMT (Katsuno et al., 2013; Moustakas and Heldin, 2014), the mediators of TGFβ1-induced EMT are still to be identified.

P21 activated kinases (Paks) are the major downstream effectors of small GTPases Rac and cdc42, which are involved in the actin-based cytoskeletal remodeling (Radu et al., 2014; Rane and Minden, 2014). We have previously shown that the pathway involving 14-3-3 adaptor proteins, Rac and Pak is important for both physiological responses to growth factors in normal cells (Somanath and Byzova, 2009) and in the promotion of invasion in prostate cancer cells (Goc et al., 2012). More recently, we demonstrated that group-I Paks such as Pak1, although not at all expressed in normal prostatic epithelial cells, is highly expressed in advanced prostate cancer patient samples and that modulation of Pak1 expression and activity in prostate cancer cells is directly linked to the changes in its tumorigenic and invasive potential (Goc et al., 2013; Schrantz et al., 2004; Yang et al., 2001). Intriguingly, we also observed an unexpected correlation between Pak1 activity and TGFβ1 expression in prostate cancer cells. Until today, the role of Pak1 in TGFβ-induced non-canonical signaling and EMT is not clear. It is more important in prostate cancer cells where Pak1 is only expressed in tumor, but not in normal prostatic epithelial cells.

In the current study, we focused on characterizing the link between TGFβ1-mediated EMT in prostate cancer cells with modulation of Pak1 activity. Our results demonstrate that although TGFβ1 induces apoptosis and tumor regression, it also stimulates Rac1 and Pak1activities in prostate cancer cells inducing cytoskeletal remodeling, expression of mesenchymal markers in the promotion of EMT, enhanced cell motility and invasion. TGFβ1-induced Pak1 activation was independent of Smad2-mediated canonical pathway and was dependent on TRAF6-mediated non-canonical pathway. Our study also is the first one to show that targeting Pak1 using IPA 3 can inhibit TGFβ1-induced prostate cancer EMT and invasion.

2. Materials and Methods

2.1. Reagents, cell lines and antibodies

Metastatic (Androgen independent) prostate cancer cell lines (PC3 and DU145) were obtained from ATCC (Manassas, VA) and maintained in DMEM-High Glucose (Hyclone, Logan, UT) with 10% FBS, 100 units/ml penicillin and 100 μg/ml streptomycin in 5% CO_2 humidified atmosphere at 37 °C. Primary antibodies against p-Pak1/2, total Pak1, p-Smad2/3, total Smad2/3, E-cadherin, N-cadherin, Vimentin, Keratin8/18, Snail, Slug, cleaved caspases 9 and 3, TGFβ1, TRAF6 and p-P38-MAPK were purchased from Cell Signaling (Boston, MA). Primary antibody against Rac1 and β-actin were purchased from Sigma-Aldrich (St Louis, MO). Anti-mouse and anti-rabbit HRP conjugated secondary antibodies were purchased from Bio-Rad (Hercules, CA). Selective Pak1 inhibitor (IPA 3) was purchased from Tocris bioscience (Minneapolis, MN). SiPak1 and control siRNAs were purchased from Cell Signaling (Boston, MA). Rh-TGFβ1 was purchased from R&D systems (Minneapolis, MN). SiTRAF6, SiSmad2 and AlexaFluor-labelled Phalloidin were purchased from Life technologies (Carlsbad, CA).

2.2. RNA interference

Fifty percent confluent PC3 and DU145 cells were transfected with either 100 nm of control, Pak1, TRAF6 or Smad2 siRNA using lipofectamine 2000 according to the manufacturer's protocol (Life technologies, Carlsbad, CA). Cells were transfected for 48 h (for SiPak1) or 72 hours (for SiSmad2 and SiTRAF6) and then subjected to treatment with TGFβ1 (5 ng/ml) or no treatment for 24 h.

2.3. Western blotting

Whole-cell or prostate tissue lysates were prepared using lysis buffer [50 mM Tris-HCl, pH 7.4, 1% Triton X-100, 150 mM NaCl, 1 mM EDTA, 2 mM Na_3VO_4, and 1× complete protease inhibitors (Roche Applied Science, Indianapolis, IN)]. The protein concentration was measured by the D_L protein assay (Bio-Rad Laboratories, Hercules, and CA). Western blot analyses were performed as described previously (Goc et al., 2013). Densitometry was done using NIH ImageJ software.

2.4. Rac1 activity assay

Rac1 activation assay was performed using a kit from Cytoskeleton (Denver, CO) as described before (Somanath and Byzova, 2009). Briefly, PC3 and DU145 cells were treated

with TGFβ1 (5 ng/ml) for 24 h and lysates were prepared. 1 mg of cell lysates were mixed in Rac lysis buffer with Glutathione-Sepharose 4B beads conjugated with the P21-binding domain (PBD) of Pak1 fused to Glutathione S-transferase. This was followed with incubation and shaking at 4°C for 1 h. after that beads were collected through centrifugation and washed 3 times using washing buffer containing 1X protease inhibitor (Roche Applied Science, IN), and three times with 1X PBS. Proteins were eluted by boiling beads in 2X Laemmli sample buffer (BioRad, Hercules, CA) for 5 min, separated on a 12% SDS–polyacrylamide gel and the amount of activated Rac1 was determined using primary antibody against Rac1 from Sigma-Aldrich (St Louis, MO).

2.5. Cell scattering assay

PC3 and DU145 cells were seeded at a low density and were allowed to grow to form small colonies. After the formation of small scattered colonies, we replaced the DMEM/HG medium with fresh medium containing 5 % FBS and cells were treated with TGFβ1 (5 ng/ml) after IPA 3 (15 μM) treatment for 1 h prior to the addition of TGFβ1. This treatment was done daily for 3 days. Cell scattering images were taken using phase contrast as well as fluorescence microscopes and the bright field images were used for quantitative analysis after selecting 4 images each per experimental group to determine the area occupied by the cells per field using NIH Image J software.

2.6. Cell migration assay

Cell migration assay (Scratch Assay) was performed as described before (Goc et al., 2013). Briefly, Both PC3 and DU145 cells were grown on 12-well plates to reach confluence and then scratches were made in the cell monolayers using 1ml pipette tips followed by treatments with TGFβ1(5 ng/ml) alone, TGFβ1 after 1h of IPA 3 treatment or IPA 3 alone (15 μM). Control cells were incubated in DMEM including 5% serum alone. Images of scratches were taken at time zero and 72 h. The rate of migration was measured using the equation ([1-T72/T0] X 100), where T72 is the area at the end point (72 h) and T0 is the area at the start time (0 h).

2.7. Transwell invasion assay

24 Transwell permeable plates support 8.0 μm polycarbonate membrane coated with Matrigel® obtained from Corning (Tewksbury, MA) were used. Briefly cells were seeded in 6 well plates and treated with either TGFβ1 (5 ng/ml), IPA 3 alone (15 μM), or combined treatment of both every day for total of 72 h. Following this, cells were detached using cell dissociation buffer (sterile 20 mM EDTA in PBS [pH 7.4]) and 5000 cells were plated on the upper chamber of the transwell plates. Upper chambers were filled with serum free medium and lower chambers were filled with DMEM/HG medium containing 20% FBS as a chemo-attractant. Cells that invaded the Matrigel® and reached the bottom layers of the top chambers after 24 h of incubation were fixed using 3.7 % paraformaldehyde then stained with 0.5% crystal violet solution. The cells were counted manually using the inverted microscope and the average was calculated from 4 random images.

2.8. TUNEL assay

The TUNEL assay for *in situ* detection of apoptosis was performed using the ApopTag® Fluorescein in Situ Apoptosis detection kit (Millipore, MA) as previously (Alhusban et al., 2014; Goc et al., 2012). Fixed frozen sections from prostate tumor xenografts were permeabilized in ethanol: acetic acid [2:1] mixture and labeled with fluorescein 12-dUTP using terminal deoxynucleotidyl transferase. Nuclei were counterstained with DAPI. Tissue sections were analyzed for apoptotic cells with localized green fluorescence using an inverted fluorescence microscope (Zeiss Axiovert100M, Carl Zeiss, Germany).

2.9. Phalloidin staining

Phalloidin immunofluorescence staining of the cells was performed as described previously (Goc et al., 2013). Briefly, PC3 or DU145 cells were plated on cell culture chamber slides (Fisher Scientific, Pittsburgh, PA) at low density were subjected to treatment with TGFβ1 (5 ng/ml) every day. After 3 days, cells were washed 2 times with 1X PBS and fixed with 1% paraformaldehyde in PBS. Cells were permeabilized using 0.1% Triton X-100 in PBS. The nonspecific staining was blocked with 2 % BSA for 1 h at room temperature. Slides were incubated with Alexa Fluor 555-labeled phalloidin for 20 min at room temperature and washed 4 times with 1X PBS. The slides were mounted with Vectashield (Vector Laboratories), and the images were taken by an inverted fluorescence microscope (Zeiss Axiovert100M, Carl Zeiss, Germany).

2.10. In vivo prostate tumor xenograft

All animal procedures listed in this article were performed as per the protocol approved by the Institutional Animal Care and Use Committee at the Charlie Norwood Veterans Affairs Medical Center, Augusta, GA (protocol # 12-06-049). PC3 cells were grown to reach 50% confluence and subjected to Adenoviral transfection to overexpress TGFβ1, control group were transfected with adenovirus expressing GFP. 24 h after transfection, cells were collected and suspended in sterile normal saline. Cell suspension (3 million cells//mouse) was injected subcutaneously (SC) in 6–8-weeks-old male nude mice (Athymic nude mice; Harlan, Indianapolis, IN). Tumor diameters were measured with digital calipers on day 7, 14, 21, and 28, and the tumor volume in mm^3 were calculated by the modified ellipsoidal formula (*Tumor volume = ½[length × width²]*) (Euhus et al., 1986). Mice were euthanized on day 28 and tumors were dissected, weighed, and snap-frozen for further western blot and immunohistochemistry analysis.

2.11. Statistical analysis

All data are presented as means ± S.E.M. to determine significant differences between treatments and control values. We have used either one way ANOVA for groups of 3 or more. Student's t test was used for studies including 2 independent groups. Statistical analysis was performed using GraphPad Prism version 6 software.

3. RESULTS

3.1. TGFβ1 overexpression or Pak1 inhibition results in reduced prostate tumor growth

We have previously reported that TGFβ1 induces apoptosis in metastatic prostate cancer cells via P38-MAPK pathway leading to activation of caspases (Al-Azayzih et al., 2012). We also showed that Pak1 inhibition leads to increased expression of TGFβ in prostate cancer cells, once again correlating with impaired prostate tumor xenograft growth and transendothelial migration (Goc et al., 2013). This suggested the existence of a feedback loop mechanism between PAK1 and TGFβ1 in prostate cancer. We first examined the effect of TGFβ1 overexpression in PC3 cells on tumor growth in athymic nude mice, and determined whether TGFβ1 overexpression will lead to inhibition of Pak1 expression or activity. Our results demonstrated that TGFβ1 overexpression inhibits prostate tumor growth, reduces tumor volume and weight, as compared to the control group (PC3 cells transfected with adenovirus encoding GFP) (Fig. 1A and B; Supplemental Fig. 1A and B). Decreased prostate tumor growth was associated with increase in prostate cancer cell apoptosis as confirmed by TUNEL staining assay (Fig. 1D). Our results also indicated that p-P38 MAPK phosphorylation, and cleaved caspase-3 and cleaved caspase-9 levels were elevated in the TGFβ1 overexpressing PC3 cells compared to control group (Fig. 1E and F). Intriguingly, we observed increased Pak1 phosphorylation (Fig. 1E) and increased expression of Snail (Figure 1G) with TGFβ1 overexpression in prostate tumor xenografts. Next, we sought to determine if pharmacological inhibition of Pak1 using a selective inhibitor IPA 3 will enhance or inhibit prostate tumor growth. Our data indicated that treatment with IPA 3 significantly inhibited the growth of prostate tumor xenografts in athymic nude mice (Fig. 2A–C). Either of the TGFβ or IPA 3 did not have any effect on mice body weight (Fig. 1C and 2D, respectively). Taken together our results indicated that although both TGFβ1 stimuli and Pak1 inhibition lead to the inhibition of prostate tumor growth *in vivo*, TGFβ1 stimuli results in increased phosphorylation of Pak1, thus suggesting a complex relationship between TGFβ1 and Pak1-mediated cytoskeletal remodeling in prostate cancer.

3.2. TGFβ1 treatment enhances Rac1-mediated Pak1 activation in prostate cancer cells

Our previous study has demonstrated the importance of 14-3-3, Rac1 and Pak1 in prostate cancer cell cytoskeletal remodeling, motility and micrometastasis (Goc et al., 2012; Goc et al., 2013), suggesting that Pak1 activity may be necessary for the acquisition of metastatic potential. The fact that TGFβ1 stimuli enhanced Pak1 phosphorylation despite inducing apoptosis in prostate tumor xenografts further complicated our view on the role of TGFβ1 and Pak1 on prostate cancer cell function. Hence we decided to further characterize the effect of TGFβ1 stimuli on the activation of Rac-Pak1 pathway in prostate cancer cells. Our analysis of PC3 and DU145 cells indicated that treatment with TGFβ1 induced Rac1 activation (Fig 3A) associated with a significant and time-dependent increase in Pak1 (Ser$^{199/204}$ and PAK2 Ser$^{192/197}$) phosphorylation (Fig. 3B and C). Our results thus confirmed that although induces apoptosis, TGFβ1 treatment in prostate cancer leads to activation of Rac1-Pak1 pathway.

3.3. TGFβ1 augments EMT in metastatic prostate cancer cells

Initial clues on the possible role of TGFβ1 on EMT came from our finding of increased Pak1 phosphorylation in the tumor lysates with TGFβ1 overexpression. Based on this, our further analysis of tumor cell lysates and PC3 cells overexpressing TGFβ1 revealed that TGFβ1 treatment induces a significant increase in the expression of EMT markers, particularly Snail and N-Cadherin (Fig. 3D–F). We then determined the direct effect of TGFβ1 on prostate cancer (PC3 and DU145) cell morphology. Based on the results of the phalloidin staining and cell scattering assays, TGFβ1 treatment (5 ng/ml) once every 24 h for a total of 72 h induced strong morphological changes (spindle-like morphology) and cell scattering (more gaps between the cells and increased area occupied by the colonies) (Fig 4A and B), which are generally associated with the EMT. In line with these morphological changes, we sought to determine the effect of TGFβ1 on EMT markers (repression of epithelial proteins accompanied with induction of mesenchymal markers proteins). TGFβ1 (5 ng/ml) treatment was associated with suppression of epithelial marker, Keratin 8 in PC3 cells (Fig. 4C). Surprisingly, while TGFβ1 decreased the expression of E-Cadherin in DU145 cells, it increased the E-Cadherin expression in PC3 cells. However, the increase in expression of other mesenchymal markers such as N-Cadherin, Snail, vimentin and slug with TGFβ1 treatment was consistent between the PC3 and DU145 cells (Fig. 4C–G and Supplemental Figure 1). Taken together, our results on the morphological and EMT marker expression profile strongly suggested that treatment with TGFβ1 induces EMT in prostate cancer cells.

3.4. Pharmacological inhibition of Pak1 reverses EMT-associated morphological changes, cell scattering, and motility in prostate cancer cells

Since Pak1-mediated cytoskeletal assembly is essential for prostate cancer cell motility, we assumed that Pak1 activation induced by TGFβ1 may be necessary for the promotion of EMT. To confirm this, we treated both PC3 and DU145 cells with a selective Pak1 inhibitor (IPA 3), which works through covalent binding to the Pak1 regulatory domain and preventing the binding of the upstream activators (Rac1/cdc42) (Viaud and Peterson, 2009). Cells treated with IPA 3 were associated with significant inhibition of TGFβ1-mediated cell scattering and morphological changes similar to mesenchymal cells (Fig. 5A and B). We next examined the role of Pak1 in TGFβ1-mediated prostate cancer migration. We subjected both PC3 and DU145 cells to cell migration (scratch recovery) after treatment with TGFβ1 (5ng/ml), IPA 3 (15 μM), or both. Treatment with IPA 3 resulted in significant inhibition of TGFβ1-mediated PC3 (Fig. 5C and D) and DU145 (Fig. 5E and F) cell migration. Our data indicated that targeting Pak1 pathway may inhibit prostate cancer EMT by TGFβ1 stimuli.

3.5. Treatment with IPA 3 reverses EMT marker expression and invasion

Since treatment with IPA 3 reversed TGFβ1-mediated morphological changes in prostate cancer cells, we next determined if inhibition of Pak1 expression has any effect on the expression of EMT markers. Our data revealed that IPA 3 significantly suppresses TGFβ1-mediated increase in the expression of mesenchymal markers N-cadherin and Snail in PC3 (Fig. 6A–C) and DU145 (Fig. 6D–F) cells. To further confirm our data, we used Pak1 siRNA to determine if these effects mediated by IPA 3 treatments were selectively dependent on Pak1 activity inhibition. Cells were transfected with either control siRNA or

Pak1 siRNA for 48 h then treated with either TGFβ1 (5 ng/ml) or vehicle (sterile PBS) for additional 24 h. siRNA-mediated Pak1 knock down blunted TGFβ1-mediated increase in EMT markers N-Cadherin and Snail in PC3 cells (Fig. 7A–C). Our results thus demonstrate that selective inhibition of Pak1 activity leads to reversion of TGFβ1-mediated EMT switch.

3.6. TGFβ1-induced Pak1 activation is dependent on non-canonical TRAF6-mediated pathway

Since TGFβ1 activates both canonical Smad-dependent (Massague, 2008) and non-canonical TRAF4/6-mediated pathway (Kalkan et al., 2009; Zhang et al., 2013), we next investigated the pathway responsible for the TGFβ1-induced Pak1 activation in prostate cancer cells. Our analysis indicated that SiRNA-mediated knockdown of Smad-2 in PC3 cells had no significant effect on the phosphorylation of Pak1 (Fig. 7D). Interestingly, SiRNA-mediated knockdown of TRAF6 in PC3 cells resulted in a significant reduction in the levels of phosphorylated Pak1 (Fig. 7E), similar to the effect of a direct SiRNA-mediated knockdown of Pak1 in PC3 cells (Fig. 7F). Our results indicate that TGFβ1-induced Pak1 activation involved a Smad2-independent, TRAF6-dependent non canonical pathway.

Acquisition of mesenchymal morphology in EMT has been linked to cancer cell invasion (Morimoto et al., 2014). Hence, we determined whether inhibition of Pak1 will affect TGFβ1-induced invasion of prostate cancer cells. To do this, we employed both pharmacological inhibition using IPA 3 and siRNA-mediated knockdown of Pak1 and then subjected these cells for a Matrigel®-based Boyden chamber invasion assay *in vitro*. Both PC3 and DU145 cells were subjected to invasion assay using Matrigel® coated transwells after the cells were treated with TGFβ1 (5ng/ml), IPA 3 (15 μM), or a combination of TGFβ1and IPA 3. Alternatively, PC3 and DU145 cells with siRNA-mediated Pak1 gene knockdown were also subjected for TGFβ1 treatment and invasion assay. Our data revealed that TGFβ1 treatment is associated with an increase in PC3 (Fig. 8A, C and E) and DU145 (Fig. 8B, D and F) prostate cancer cell invasion, and these effects were significantly abolished by suppression Pak1 activity using either IPA 3 or siRNA mediated gene silencing (Fig 8). Together, our data demonstrate that Pak1 activation upon TGFβ1 stimuli via TRAF6-mediated non-canonical pathway is important for prostate cancer EMT.

4. DISCUSSION

Previous studies have demonstrated the central role of TGFβ1 in EMT as characterized by the reduced epithelial marker expression, increased mesenchymal marker expression, loss of cell-cell contacts and increased cell motility/invasion leading to cancer metastasis (Nauseef and Henry, 2011; Thiery et al., 2009). However, mechanism by which TGFβ1 promotes EMT is still not clear. We have previously demonstrated that 14-3-3ζ-Rac1 signaling pathway, an upstream modulator of Group I Paks including Pak1 is necessary for prostate cancer cell (LNCaP and PC3) motility and transendothelial migration (Goc et al., 2012). We also demonstrated that P21-activated kinase 1 (Pak1) is highly expressed in metastatic prostate cancer cells (PC3, LNCaP C4-2 and VCaP) compared to the non-metastatic cells (LNCaP) and that Pak1 expression is highly elevated in metastatic prostate cancer tissues compared to normal and benign prostatic hyperplasia tissues. Interestingly, our previous study also indicated that Pak1 enhances prostate tumor xenograft growth via down

regulating TGFβ expression (Goc et al., 2013). Literature supports that Pak1 signaling is essential for EMT process in various epithelial cells (Jin et al., 2014; Lv et al., 2013; Sebe et al., 2008). However, role of Pak1 in cancer EMT, more particularly in the prostate, where Pak1 is expressed only in cancer is not clear. Hence, in the current study, we focused on characterizing the link between the TGFβ1 and Pak1 in prostate cancer and unveil the signaling upstream and downstream of Pak1 activation by TGFβ1 in the promotion of EMT.

In various cancers such as Breast (Arias-Romero et al., 2013; Rider et al., 2013), lung (Rettig et al., 2012) and renal cell carcinoma (O'Sullivan et al., 2007), group I Paks, Pak1 in particular, have been implicated in the promotion of oncogenic transformation, tumor progression and metastasis (Kichina et al., 2010; Radu et al., 2014). Research on the role of group I Paks in prostate cancer has been hampered due to the reason that group I Paks are not abundantly expressed in the normal prostate gland, and is absent in prostatic epithelial cells (Goc et al., 2013). Instead, prostate gland expresses high levels of group II Paks, Pak4 and Pak6 (Ahmed et al., 2008; Park et al., 2013; Schrantz et al., 2004). Intriguingly, it was not clear what mediated cytoskeletal changes in prostate cancer cells, which is essential for the acquisition of invasive and metastatic potential by prostate cancer cells. It is known that group II Paks has no Rac1 binding PBD region, and that regulation of group II Pak activity is independent of Rac1 and cdc42 activation (Kichina et al., 2010). This suggested that although group I Paks are expressed in low amounts in the prostate gland, its enhanced expression and activation may be necessary for the promotion of prostate cancer EMT by TGFβ1.

Although an association between group I Paks and invasion was not established in prostate cancer cells, there were reports supporting possibility of such an association (Even-Faitelson et al., 2005). Our follow up study identified that although Pak1 is not highly expressed in low grade prostate cancer cell lines and in normal human prostate or benign prostatic hyperplasia tissue samples; its expression was higher in metastasized tissues including lymph node and lungs (Goc et al., 2013). Increased expression of Pak1 was also observed in aggressive human prostate cancer cell lines (Goc et al., 2013). We also confirmed that inhibition of Pak1 via shRNA-mediated gene silencing leads to growth inhibition of PC3 tumor xenograft in nude mice (Goc et al., 2013). Interestingly, this was accompanied with an increase in the expression of TGFβ in the PC3 tumor xenografts, thus suggesting that there is a likely existence of a Pak1-TGFβ signaling loop thus promoting tumor progression and invasion.

Since TGFβ is a well-known tumor suppressor in prostate cancer cells (Al-Azayzih et al., 2012; Edlund et al., 2003; Hayes et al., 2001; Yoo et al., 2009), we assumed that increased TGFβ expression due to Pak1 inhibition may have an effect on the inhibition of tumor growth in addition to the effect of Pak1 inhibition on cytoskeletal remodeling in prostate cancer cells.

However, recent literature also indicates that TGFβ switches its role to promote metastasis in advanced prostate tumors (Morimoto et al., 2014; Thakur et al., 2014). This complicated our view on how TGFβ and Pak1 may be associated in the promotion of prostate cancer cell invasion. Our results indicated that TGFβ1 overexpression in PC3 prostate tumor xenografts

induced apoptosis mainly through the activation of stress-activated p38-MAPK pathway, thus confirming the predominant role of TGFβ1 as a tumor suppressor (Al-Azayzih et al., 2012; Nastiuk et al., 2008; Pu et al., 2009; Song et al., 2010; Yoo et al., 2009). Surprisingly, TGFβ1 overexpression resulted in significantly increased active Rac1 and phosphorylated Pak1/2 accompanied by increased expression of a mesenchymal markers Snail and N-Cadherin. These results suggested that while TGFβ1 acts predominantly as a prostate tumor growth suppressor via inducing apoptosis, it concurrently induced phenotypic switching and expression of mesenchymal markers in a subgroup of prostate cancer cells. Prolonged stimulation of prostate cancer cells with TGFβ1 resulted in EMT, characterized by morphological changes, increased cell scattering, loss of cell-cell contacts, loss in epithelial markers, and acquisition of mesenchymal markers. These results were in agreement with the literature that despite being a tumor suppressor early on, prolonged TGFβ1 stimuli can promote EMT and enhance invasiveness of the prostate cancer cells (Nauseef and Henry, 2011; Thiery et al., 2009)

It is known that both canonical Smad-dependent and non-canonical pathways are necessary for the TGFβ-induced effects on epithelial cells (Massague, 2008, 2012). Although not proven, scientists argue that while canonical pathway is responsible for the tumor suppressive effect of TGFβ, EMT-promoting effects of TGFβ is dependent on the activation of non-canonical pathways leading to activation of small Rho-GTPases such as Rac1 and cdc42 (Makrodouli et al., 2011). Our results showed that TGFβ1-induced Pak1 activation is independent of canonical Smad2-pathway and is dependent on the non-canonical TRAF6 pathway.

Although we established that Rac1 and Pak1 activities is essential for cytoskeletal remodeling in prostate cancer cells, there are no reports indicating the potential role of Rac1-Pak1 pathway in TGFβ1-induced EMT in prostate cancer cells. Our study also revealed for the first time that prolonged treatment of prostate cancer cells with TGFβ1 results in increased activation of Rac1 and Pak1. Pak1 deficient PC3 cells were resistant to TGFβ1-promoted EMT and invasion of prostate cancer cells. IPA 3, a selective allosteric Pak1 inhibitor was able to reverse TGFβ1-associated EMT suggesting the indispensable role of "Rac1-Pak1" axis in TGFβ1-mediated cytoskeletal remodeling and EMT. Pak1 deficient PC3 cells were resistant to TGFβ1-promoted EMT and invasion of prostate cancer cells. In conclusion, we show for the first time that TGFβ1 induces cytoskeletal remodeling, EMT, invasion and metastasis via regulation of "Rac1-Pak1 axis". These results suggest that targeting this axis could be a potential treatment target for the advanced-stage prostate cancer.

Supplementary Material

Refer to Web version on PubMed Central for supplementary material.

Acknowledgments

References

1. Ahmed T, Shea K, Masters JR, Jones GE, Wells CM. A PAK4-LIMK1 pathway drives prostate cancer cell migration downstream of HGF. Cell Signal. 2008; 20:1320–1328. [PubMed: 18424072]

2. Akhurst RJ, Derynck R. TGF-beta signaling in cancer--a double-edged sword. Trends Cell Biol. 2001; 11:S44–51. [PubMed: 11684442]

3. Al-Azayzih A, Gao F, Goc A, Somanath PR. TGFbeta1 induces apoptosis in invasive prostate cancer and bladder cancer cells via Akt-independent, p38 MAPK and JNK/SAPK-mediated activation of caspases. Biochem Biophys Res Commun. 2012; 427:165–170. [PubMed: 22989755]

4. Alhusban A, Al-Azayzih A, Goc A, Gao F, Fagan SC, Somanath PR. Clinically relevant doses of candesartan inhibit growth of prostate tumor xenografts in vivo through modulation of tumor angiogenesis. J Pharmacol Exp Ther. 2014; 350:635–645. [PubMed: 24990940]

5. Arias-Romero LE, Villamar-Cruz O, Huang M, Hoeflich KP, Chernoff J. Pak1 kinase links ErbB2 to beta-catenin in transformation of breast epithelial cells. Cancer Res. 2013; 73:3671–3682. [PubMed: 23576562]

6. Edlund S, Bu S, Schuster N, Aspenstrom P, Heuchel R, Heldin NE, ten Dijke P, Heldin CH, Landstrom M. Transforming growth factor-beta1 (TGF-beta)-induced apoptosis of prostate cancer cells involves Smad7-dependent activation of p38 by TGF-beta-activated kinase 1 and mitogen-activated protein kinase kinase 3. Mol Biol Cell. 2003; 14:529–544. [PubMed: 12589052]

7. Euhus DM, Hudd C, LaRegina MC, Johnson FE. Tumor measurement in the nude mouse. J Surg Oncol. 1986; 31:229–234. [PubMed: 3724177]

8. Even-Faitelson L, Rosenberg M, Ravid S. PAK1 regulates myosin II-B phosphorylation, filament assembly, localization and cell chemotaxis. Cell Signal. 2005; 17:1137–1148. [PubMed: 15993754]

9. Gheldof A, Berx G. Cadherins and epithelial-to-mesenchymal transition. Prog Mol Biol Transl Sci. 2013; 116:317–336. [PubMed: 23481201]

10. Goc A, Abdalla M, Al-Azayzih A, Somanath PR. Rac1 activation driven by 14-3-3zeta dimerization promotes prostate cancer cell-matrix interactions, motility and transendothelial migration. PLoS One. 2012; 7:e40594. [PubMed: 22808202]

11. Goc A, Al-Azayzih A, Abdalla M, Al-Husein B, Kavuri S, Lee J, Moses K, Somanath PR. P21 activated kinase-1 (Pak1) promotes prostate tumor growth and microinvasion via inhibition of transforming growth factor beta expression and enhanced matrix metalloproteinase 9 secretion. J Biol Chem. 2013; 288:3025–3035. [PubMed: 23258534]

12. Gupta GP, Massague J. Cancer metastasis: building a framework. Cell. 2006; 127:679–695. [PubMed: 17110329]

13. Hayes SA, Zarnegar M, Sharma M, Yang F, Peehl DM, ten Dijke P, Sun Z. SMAD3 represses androgen receptor-mediated transcription. Cancer Res. 2001; 61:2112–2118. [PubMed: 11280774]

14. Inman GJ. Switching TGFbeta from a tumor suppressor to a tumor promoter. Curr Opin Genet Dev. 2011; 21:93–99. [PubMed: 21251810]

15. Jin R, Liu W, Menezes S, Yue F, Zheng M, Kovacevic Z, Richardson DR. The metastasis suppressor, NDRG1, modulates beta-Catenin phosphorylation and nuclear translocation by mechanisms involving FRAT1 and PAK4. J Cell Sci. 2014

16. Kalkan T, Iwasaki Y, Park CY, Thomsen GH. Tumor necrosis factor-receptor-associated factor-4 is a positive regulator of transforming growth factor-beta signaling that affects neural crest formation. Mol Biol Cell. 2009; 20:3436–3450. [PubMed: 19458200]

17. Katsuno Y, Lamouille S, Derynck R. TGF-beta signaling and epithelial-mesenchymal transition in cancer progression. Curr Opin Oncol. 2013; 25:76–84. [PubMed: 23197193]

18. Kichina JV, Goc A, Al-Husein B, Somanath PR, Kandel ES. PAK1 as a therapeutic target. Expert Opin Ther Targets. 2010; 14:703–725. [PubMed: 20507214]

19. Kokkinos MI, Wafai R, Wong MK, Newgreen DF, Thompson EW, Waltham M. Vimentin and epithelial-mesenchymal transition in human breast cancer--observations in vitro and in vivo. Cells Tissues Organs. 2007; 185:191–203. [PubMed: 17587825]

20. Lv Z, Hu M, Zhen J, Lin J, Wang Q, Wang R. Rac1/PAK1 signaling promotes epithelial-mesenchymal transition of podocytes in vitro via triggering beta-catenin transcriptional activity under high glucose conditions. Int J Biochem Cell Biol. 2013; 45:255–264. [PubMed: 23153508]

21. Makrodouli E, Oikonomou E, Koc M, Andera L, Sasazuki T, Shirasawa S, Pintzas A. BRAF and RAS oncogenes regulate Rho GTPase pathways to mediate migration and invasion properties in human colon cancer cells: a comparative study. Mol Cancer. 2011; 10:118. [PubMed: 21943101]

22. Malvezzi M, Bertuccio P, Levi F, La Vecchia C, Negri E. European cancer mortality predictions for the year 2014. Ann Oncol. 2014

23. Massague J. TGFbeta in Cancer. Cell. 2008; 134:215–230. [PubMed: 18662538]

24. Massague J. TGFbeta signalling in context. Nat Rev Mol Cell Biol. 2012; 13:616–630. [PubMed: 22992590]

25. Morimoto K, Tanaka T, Nitta Y, Ohnishi K, Kawashima H, Nakatani T. NEDD9 crucially regulates TGF-beta-triggered epithelial-mesenchymal transition and cell invasion in prostate cancer cells: involvement in cancer progressiveness. Prostate. 2014; 74:901–910. [PubMed: 24728978]

26. Morrison CD, Parvani JG, Schiemann WP. The relevance of the TGF-beta Paradox to EMT-MET programs. Cancer Lett. 2013; 341:30–40. [PubMed: 23474494]

27. Moustakas A, Heldin CH. Non-Smad TGF-beta signals. J Cell Sci. 2005; 118:3573–3584. [PubMed: 16105881]

28. Moustakas A, Heldin P. TGFbeta and matrix-regulated epithelial to mesenchymal transition. Biochim Biophys Acta. 2014

29. Mu Y, Gudey SK, Landstrom M. Non-Smad signaling pathways. Cell Tissue Res. 2012; 347:11–20. [PubMed: 21701805]

30. Nastiuk KL, Yoo K, Lo K, Su K, Yeung P, Kutaka J, Danielpour D, Krolewski JJ. FLICE-like inhibitory protein blocks transforming growth factor beta 1-induced caspase activation and apoptosis in prostate epithelial cells. Mol Cancer Res. 2008; 6:231–242. [PubMed: 18314484]

31. Nauseef JT, Henry MD. Epithelial-to-mesenchymal transition in prostate cancer: paradigm or puzzle? Nat Rev Urol. 2011; 8:428–439. [PubMed: 21691304]

32. O'Sullivan GC, Tangney M, Casey G, Ambrose M, Houston A, Barry OP. Modulation of p21-activated kinase 1 alters the behavior of renal cell carcinoma. Int J Cancer. 2007; 121:1930–1940. [PubMed: 17621631]

33. Park MH, Lee HS, Lee CS, You ST, Kim DJ, Park BH, Kang MJ, Heo WD, Shin EY, Schwartz MA, Kim EG. p21-Activated kinase 4 promotes prostate cancer progression through CREB. Oncogene. 2013; 32:2475–2482. [PubMed: 22710715]

34. Principe DR, Doll JA, Bauer J, Jung B, Munshi HG, Bartholin L, Pasche B, Lee C, Grippo PJ. TGF-beta: duality of function between tumor prevention and carcinogenesis. J Natl Cancer Inst. 2014; 106:djt369. [PubMed: 24511106]

35. Pu H, Collazo J, Jones E, Gayheart D, Sakamoto S, Vogt A, Mitchell B, Kyprianou N. Dysfunctional transforming growth factor-beta receptor II accelerates prostate tumorigenesis in the TRAMP mouse model. Cancer Res. 2009; 69:7366–7374. [PubMed: 19738062]

36. Radu M, Semenova G, Kosoff R, Chernoff J. PAK signalling during the development and progression of cancer. Nat Rev Cancer. 2014; 14:13–25. [PubMed: 24505617]

37. Rane C, Minden A. P21 activated kinases: Structure, regulation, and functions. Small GTPases. 2014; 5

38. Rettig M, Trinidad K, Pezeshkpour G, Frost P, Sharma S, Moatamed F, Tamanoi F, Mortazavi F. PAK1 kinase promotes cell motility and invasiveness through CRK-II serine phosphorylation in non-small cell lung cancer cells. PLoS One. 2012; 7:e42012. [PubMed: 22848689]

39. Rider L, Oladimeji P, Diakonova M. PAK1 regulates breast cancer cell invasion through secretion of matrix metalloproteinases in response to prolactin and three-dimensional collagen IV. Mol Endocrinol. 2013; 27:1048–1064. [PubMed: 23744893]

40. Schrantz N, da Silva Correia J, Fowler B, Ge Q, Sun Z, Bokoch GM. Mechanism of p21-activated kinase 6-mediated inhibition of androgen receptor signaling. J Biol Chem. 2004; 279:1922–1931. [PubMed: 14573606]

41. Sebe A, Masszi A, Zulys M, Yeung T, Speight P, Rotstein OD, Nakano H, Mucsi I, Szaszi K, Kapus A. Rac, PAK and p38 regulate cell contact-dependent nuclear translocation of myocardin-related transcription factor. FEBS Lett. 2008; 582:291–298. [PubMed: 18154735]

42. Shi Y, Massague J. Mechanisms of TGF-beta signaling from cell membrane to the nucleus. Cell. 2003; 113:685–700. [PubMed: 12809600]

43. Siegel R, Ma J, Zou Z, Jemal A. Cancer statistics, 2014. CA Cancer J Clin. 2014; 64:9–29. [PubMed: 24399786]

44. Smith BN, Odero-Marah VA. The role of Snail in prostate cancer. Cell Adh Migr. 2012; 6:433–441. [PubMed: 23076049]

45. Somanath PR, Byzova TV. 14-3-3beta-Rac1-p21 activated kinase signaling regulates Akt1-mediated cytoskeletal organization, lamellipodia formation and fibronectin matrix assembly. J Cell Physiol. 2009; 218:394–404. [PubMed: 18853424]

46. Song K, Wang H, Krebs TL, Wang B, Kelley TJ, Danielpour D. DHT selectively reverses Smad3-mediated/TGF-beta-induced responses through transcriptional down-regulation of Smad3 in prostate epithelial cells. Mol Endocrinol. 2010; 24:2019–2029. [PubMed: 20739403]

47. Thakur N, Gudey SK, Marcusson A, Fu JY, Bergh A, Heldin CH, Landstrom M. TGFbeta-induced invasion of prostate cancer cells is promoted by c-Jun-dependent transcriptional activation of Snail1. Cell Cycle. 2014; 13

48. Thiery JP, Acloque H, Huang RY, Nieto MA. Epithelial-mesenchymal transitions in development and disease. Cell. 2009; 139:871–890. [PubMed: 19945376]

49. Viaud J, Peterson JR. An allosteric kinase inhibitor binds the p21-activated kinase autoregulatory domain covalently. Mol Cancer Ther. 2009; 8:2559–2565. [PubMed: 19723886]

50. Yang F, Li X, Sharma M, Zarnegar M, Lim B, Sun Z. Androgen receptor specifically interacts with a novel p21-activated kinase, PAK6. J Biol Chem. 2001; 276:15345–15353. [PubMed: 11278661]

51. Yoo KS, Nastiuk KL, Krolewski JJ. Transforming growth factor beta1 induces apoptosis by suppressing FLICE-like inhibitory protein in DU145 prostate epithelial cells. Int J Cancer. 2009; 124:834–842. [PubMed: 19048627]

52. Zarzynska JM. Two Faces of TGF-Beta1 in Breast Cancer. Mediators Inflamm. 2014; 2014:141747. [PubMed: 24891760]

53. Zhang L, Zhou F, Garcia de Vinuesa A, de Kruijf EM, Mesker WE, Hui L, Drabsch Y, Li Y, Bauer A, Rousseau A, Sheppard KA, Mickanin C, Kuppen PJ, Lu CX, Ten Dijke P. TRAF4 promotes TGF-beta receptor signaling and drives breast cancer metastasis. Mol Cell. 2013; 51:559–572. [PubMed: 23973329]

Author Manuscript

Author Manuscript

Author Manuscript

Author Manuscript

HIGHLIGHTS

- The role of Pak1 in epithelial to mesenchymal transition is unclear.

- TGFβ1/Pak1/TRAF6 pathway mediates prostate cancer epithelial to mesenchymal transition

- Pak1 is a potential target for the treatment of advanced prostate cancer
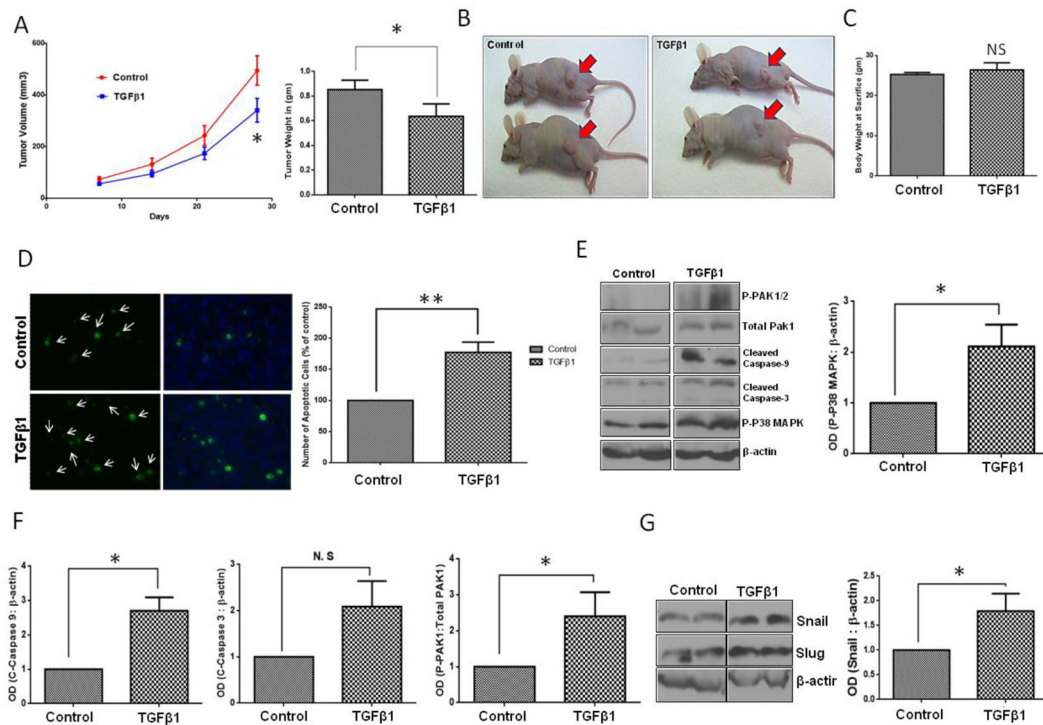
Figure 1. TGFβ1 overexpression results in the growth inhibition of prostate tumor xenografts
A. Figure showing tumor volume (left) and weight (right) analysis of the PC3 tumor xenografts bearing either Ad-GFP or Ad-TGFβ1 overexpression. B. Representative images of xenograft tumor in both control and TGFβ1 overexpression groups (n= 6) C. Bar graph representing mice body weight on the date of tumor collection. D. Pictures showing TUNEL staining (green), DAPI (blue) and bar graph indicating prostate cancer cell apoptosis in tumor xenograft sections taken from either control or TGFβ1 overexpressing tumors (n= 6). E. Western blot images of control and Ad-TGFβ1 expressing PC3 tumor xenograft lysates showing expression levels of p-p38 MAPK, cleaved caspase 3, cleaved caspase 9, p-PAK1, and total PAK1 normalized to β-actin (left) and bar graph representing optical densitometry measurements of p-p38-MAPK expression normalized to β-actin (right) (n= 4). F. Bar graphs representing optical densitometry measurements of cleaved caspase-9, cleaved caspase-3 and phosphorylated Pak1expressions in prostate tumor xenografts normalized to β-actin (n= 3). G. Western blot image of Snail and slug expressions in prostate tumor xenografts (left) and bar graph representing optical densitometry measurements of Snail expression (right) normalized to β-actin (n= 3).*$p<0.05$ and **$P<0.01$, Data presented as Mean ± SEM.
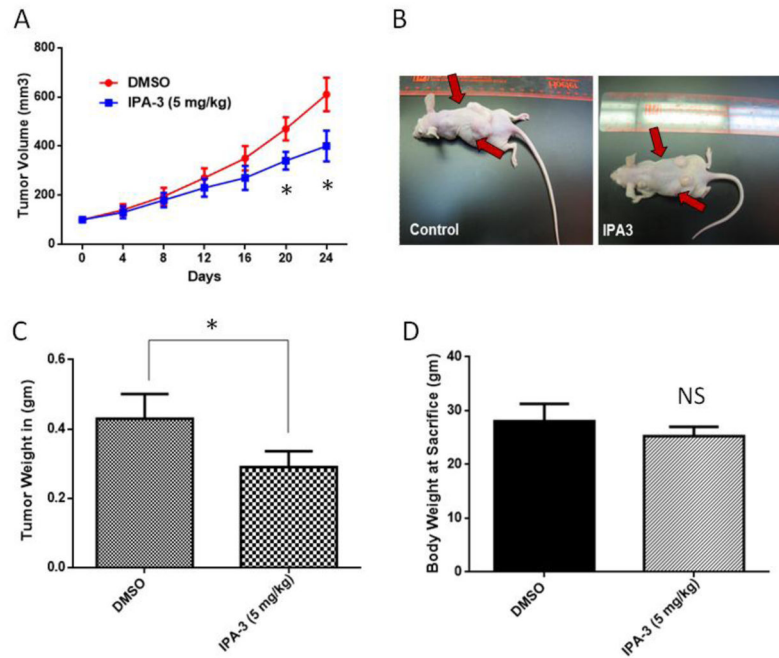
Figure 2. Treatment with IPA 3 results in the growth inhibition of prostate tumor xenografts
A. Panel showing tumor volume measurements from Day 0 to Day 24 (left) and representative pictures of tumor xenograft from DMSO or IPA 3 (5mg/Kg) treatments groups on Day 24 (n= 4–5) (right). B. Bar graph showing weights of tumors from mice treated with either DMSO or IPA 3 (5mg/Kg) collected on Day 24. C. Bar graph representing mice body weight on the date of tumor collection. (n= 4–5). *$p<0.05$ and **$P<0.01$, Data presented as Mean ± SEM.
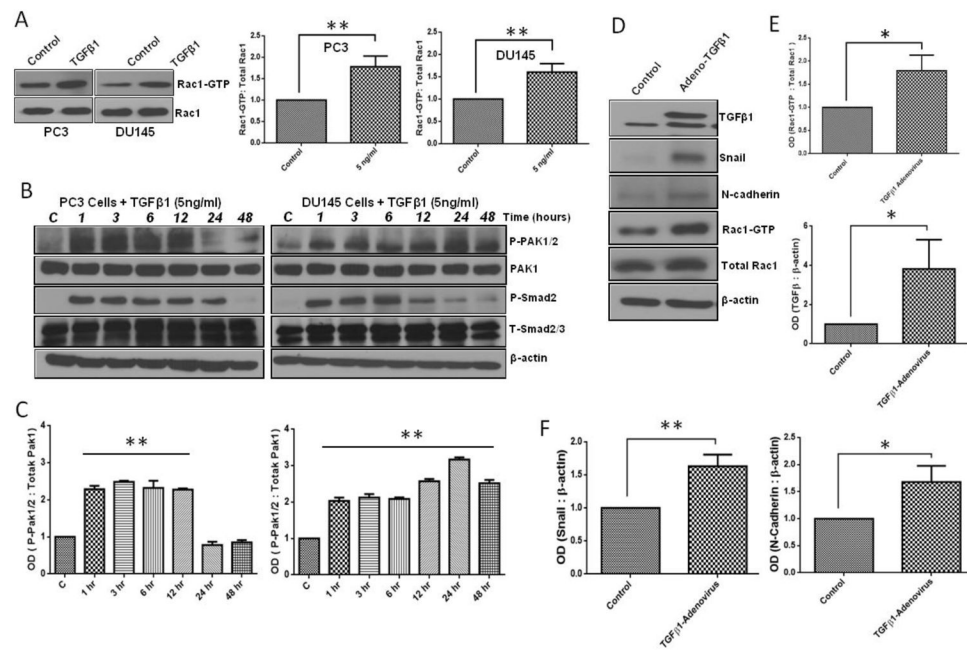
Figure 3. TGFβ1 treatment enhances Rac1-mediated Pak1 activation and expression of mesenchymal markers (Snail and N-cadherin) in prostate cancer cells

A. Western blot images of active Rac1 (Rac1-GTP) bands after one time treatments with TGFβ1 (5ng/ml) or control vehicle in PC3 and DU145 cells (left) and Bar graphs showing band densitometry analysis of Rac1-GTP expressions normalized to β-actin after treatment of PC3 and DU145 cells with or without TGFβ1 (5 ng/ml) for 24 h (right) (n= 4). B. Representative Western blot images of P-PAK1/2, Total Pak1, P-smad2/3, T-Smad after one time treatments with TGFβ1 (5ng/ml) or vehicle for 1, 3, 6, 12, 24 and 48 h in PC3 and DU145 cells. C. Bar graphs showing band densitometry analysis P-PAK1/2 normalized to total Pak1 after treatment with TGFβ1 (5ng/ml) or PBS for 1, 3, 6, 12, 24 and 48 h in PC3 and DU145 cells, respectively (n= 4). D. Representative Western blot images of EMT marker expression and active Rac1-GTP in PC3 cells after being subjected to infection with either control Ad-GFP or Ad-TGFβ1. E. Bar graphs representing optical densitometry measurements for Rac1-GTP and TGFβ expression levels in PC3 cells after 48 h post transfection (n= 4). E. Bar graphs representing optical densitometry measurements of Snail and N-cadherin expressions, respectively, in PC3 cells 48 h post-transfection with Ad-GFP or Ad-TGFβ1 (n= 4). *$p<0.05$ and **$P<0.01$, Data presented as Mean ± SEM.
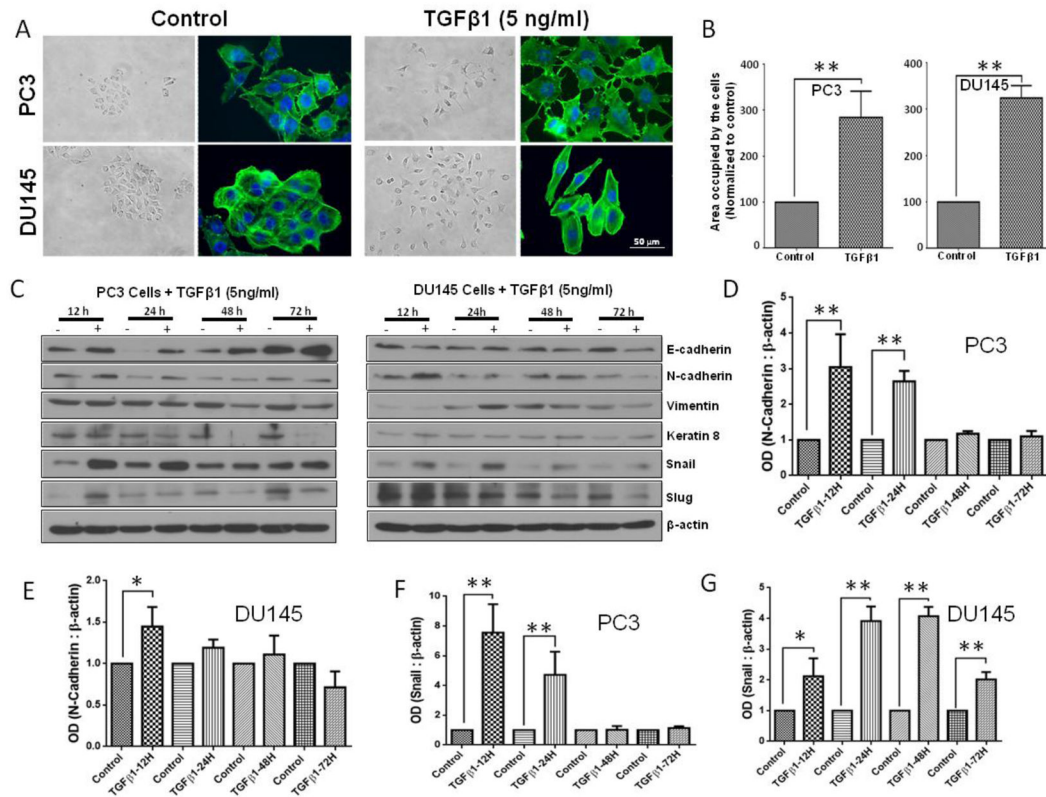
Figure 4. TGFβ1 enhances Snail and N-cadherin expression, and EMT in prostate cancer cells
A. Representative images showing the effect of TGFβ1 (5 ng/ml for 3 days) on stress fiber formation (phalloidin staining) in PC3 and DU145 cells (x 40 magnification) and phase-contrast images showing the effect of TGFβ1 (5 ng/ml) on cell scattering in both cell lines (x 20 magnification). B. Bar graphs showing quantification of the cell scattering data in PC3 (left) and DU145 (right) cells (n= 4). C. Representative Western blot images of E-Cadherin, Keratin 8, N-cadherin, Vimentin, Snail, and Slug after one time treatment with TGFβ1 (5ng/ml) or no treatment for 12, 24, 48, and 72 h in PC3 and DU145 cells. D. Bar graph showing optical band densitometry analysis of N-cadherin expression in PC3 cells, after one time treatment with TGFβ1 (5ng/ml) or no treatment for 12, 24, 48, and 72 h normalized to β-actin (n= 4). E. Bar graph showing optical band densitometry analysis of N-cadherin expression in DU145 cells, after one time treatment with TGFβ1 (5ng/ml) or no treatment for 12, 24, 48, and 72 h normalized to β-actin (n= 4). F. Bar graph showing optical band densitometry analysis of Snail expression in PC3 cells, after treatments with TGFβ1 (5ng/ml) or no treatment for 12, 24, 48, and 72 h normalized to β-actin (n= 4). G. Bar graph showing optical band densitometry analysis of Snail expression in DU145 cells, after treatments with TGFβ1 (5ng/ml) or no treatment for 12, 24, 48, and 72 h normalized to β-actin (n= 4). *$p<0.05$ and **$P<0.01$, Data presented as Mean ± SEM.
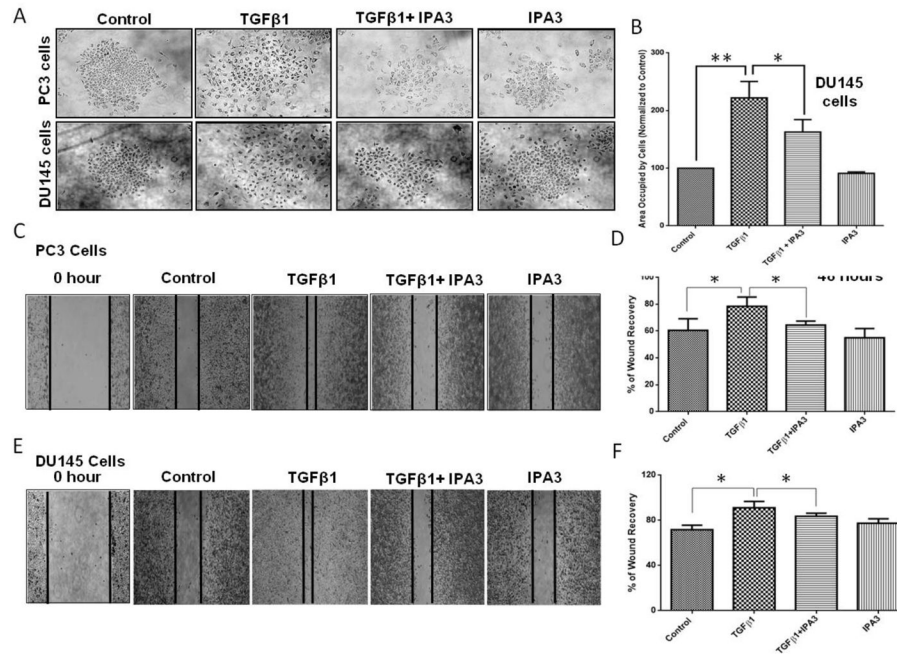
Figure 5. Pharmacological inhibition of Pak1 with IPA 3 inhibits TGFβ1-induced EMT-associated morphological changes, cell scattering, and motility in prostate cancer cells
A. Representative images of PC3 and DU145 cell scattering following 72 h treatments with TGFβ1 (5 ng/ml), or IPA 3 (15 μM), or a combination. B. Bar graph showing quantification of the cell scattering in DU145 cells as treated above (n= 4). C and D. Representative images and bar graph of PC3 cell migration following 48 h treatments of TGFβ1 (5 ng/ml), IPA 3 (15 μM), or a combination (n= 4). E and F. Representative images and bar graph of DU145 cell migration following 48 h treatments of TGFβ1 (5 ng/ml), IPA 3 (15 μM), or a combination (n= 4). *$p<0.05$ and **$P<0.01$, Data presented as Mean ± SEM.
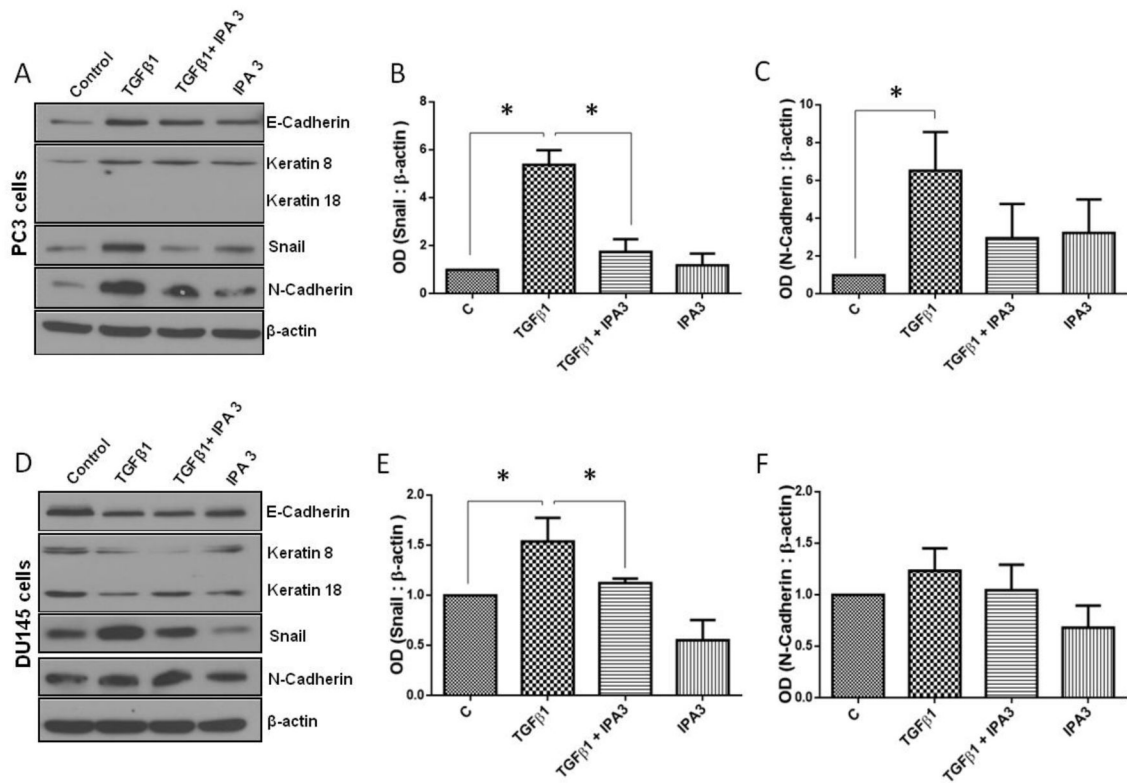
Figure 6. IPA 3, Selective Pak1 inhibitor inhibits TGFβ1-mediated EMT in prostate cancer cells
A, Representative Western blot images of EMT marker expression in PC3 cells following 72 h treatments with TGFβ1 (5 ng/ml), IPA 3 (15 μM), or combination, with treatments repeated every 24 hours. B and C. Bar graph representing optical densitometry for mesenchymal markers, Snail and N-Cadherin expressions respectively in PC3 cells following 72 h treatments with TGFβ1 (5 ng/ml), IPA 3 (15 μM), or combination (n= 3). D, Representative Western blot images of EMT markers expression in DU145 cells following 72 h treatments with TGFβ1 (5 ng/ml), IPA 3 (15 μM), or combination. E and F. Bar graph representing optical densitometry of mesenchymal markers, Snail and N-Cadherin expressions respectively in DU145 cells following 72 h treatments with TGFβ1 (5 ng/ml), IPA 3 (15 μM), or combination (n= 3). *$p<0.05$, Data presented as Mean ± SEM.
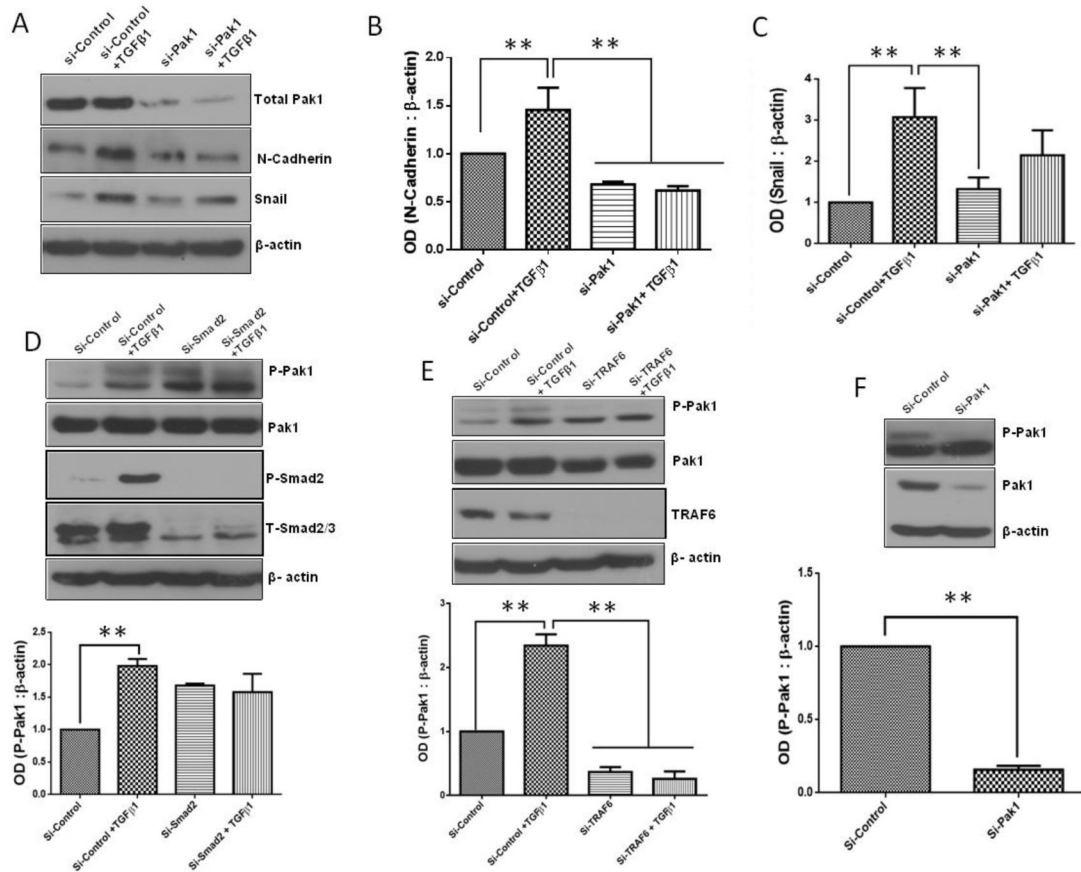
Figure 7. Selective Pak1 knockdown in PC3 cells inhibits EMT marker expression induced by TGFβ1 treatment involving TRAF6 pathway

A. Representative Western blot images showing EMT marker expression in PC3 cells after being subjected to either control siRNA or Pak1 siRNA for 48 h followed by treatment with or without TGFβ1 (5ng/ml) for 24 h. B and C. Bar graphs representing optical densitometry measurements for mesenchymal marker expression (N-Cadherin and Snail, respectively) in either Control-siRNA or Pak1 siRNA transfected PC3 cells (n= 3). D. Representative Western blot images and bar graph showing changes in the phosphorylation of Pak1 with the Si-RNA-mediated knockdown of Smad2 for 48 h followed by treatment with or without TGFβ1 (5ng/ml) for 24 h in PC3 cells, compared to Si-Control (n= 3). E. Representative Western blot images bar graph showing optical densitometry measurements for phosphorylated Pak1 in Control-siRNA or TRAF6 SiRNA transfected PC3 cells (n= 3). F. Representative Western blot image and bar graph showing changes in the Pak1 phosphorylation in PC3 cells with Pak1 knockdown (n= 3).*$p<0.05$ and **$P<0.01$, Data presented as Mean ± SEM.
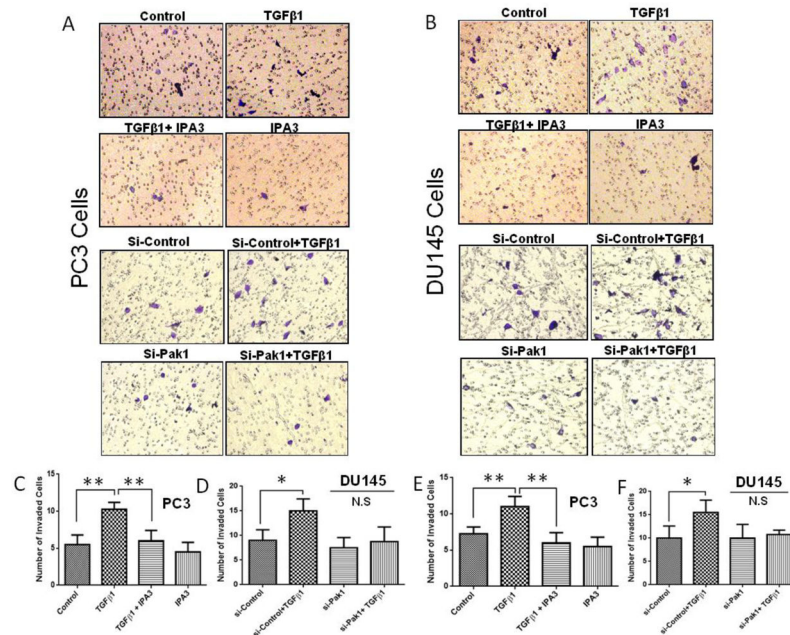
Figure 8. IPA-3, Selective Pak1 inhibitor or Pak1 knockdown prevents TGFβ1-mediated prostate cancer cells invasion

A. Representative images of transwell plates following invasion assay of PC3 cells subjected to either IPA 3 treatment or Pak1 knockdown. B, Representative images of transwell plates following invasion assay of DU145 cells after subjected to either IPA 3 treatment or Pak1 knockdown. C and D. Bar graphs showing PC3 cell invasion (cells/field) after either IPA 3 treatment or Pak1 knockdown (n= 4). E and F, Bar graphs showing DU145 cell invasion (cells/field) after subjected to either IPA 3 treatment or Pak1 knockdown (n= 4). *$p<0.05$ and **$P<0.01$, Data presented as Mean ± SEM.